Three dimensional analysis of chromatic aberration in diffractive elements with extended depth of focus

D. Mas*, J. Espinosa, J. Perez, and C. Illueca

[1]*Dept. Optica, Univ. Alicante. Carretera San Vicente del Raspeig s/n - 03690 San Vicente del Raspeig Alicante Spain*

**Corresponding author: david.mas@ua.es*

Abstract: The paper presents the polychromatic analysis of two diffractive optical elements with extended depth of focus: the linear axicon and the light sword optical element. Chromatic aberration produces axial displacement of the focal segment line. Thus, we explore the possibility of extending the focal depth of these elements to permit superposition of the chromatic foci. In the case of an axicon, we achieve an achromatic zone where focusing is produced. In the case of the light sword element, we show that the focusing segment is out of axis. Therefore a superposition of colors is produced, but not on axis overlapping. Instead, three colored and separated foci are simultaneously obtained in a single plane. Three dimensional structures of the propagated beams are analyzed in order to provide better understanding of the properties and applications of such elements.

OCIS codes: (050.1970) Diffractive optics; (120.3620) Lens system design; (110.4100) Modulation transfer function

References

1. J. Sochacki, A. Kolodziejczyk, Z. Jaroszewicz and S. Bara, "Non paraxial design of generalized axicons," Appl. Opt. **31,** 5326-5330 (1992).
2. A. Kolodziejczyk, S. Bara, Z. Jaroszewicz, M. Sypek, "The light sword optical element -a new diffraction structure with extended depth of focus," J. Mod. Opt. **37,** 1283-1286 (1990).
3. Z. Jaroszewicz and J. Morales, "Lens axicons: systems composed of a diverging aberrated lens and a converging aberrated lens," J. Opt. Soc. Am. A **16**, 191-197 (1999).
4. A: Burvall, K. Kolacz, Z. Jaroszewicz and A. Friberg, "Simple lens axicon," Appl. Opt. **43,** 4838-4844 (2004).
5. A. Flores, M. Wang and J. J. Yang, "Achromatic hybrid refractive-diffractive lens with extended focal length," Appl. Opt. **43,** 5618-5630 (2004).
6. J. Monsoriu, W. Furlan, P. Andres and J. Lancis, "Fractal conical lenses," Opt. Express **14,** 9077-9082 (2006).
7. C. Iemmi, J. Campos, J. C. Escalera, O. Lopez-Coronado, R. Gimeno and M. J. Yzuel, "Depth of focus increase by multiplexing programmable diffractive lenses," Opt. Express **14,** 10207-10217 (2006).
8. J. Leach, G. M. Gibson, M. Padgett, E. Exposito, G. McConell, A. J. Wright and J. M. Girkin, "Generation of achromatic Bessel beams using a compensated spatial light modulator," Opt. Express **14**, 5581-5587 (2006),
9. I. Golub, "Fresnel axicon," Opt. Lett. **31,** 1890-1892 (2006).
10. Z. Zalevski and S. Ben-Yaish, "Extended depth of focus imaging with birefringent plate," Opt. Express **15,** 7202-7209 (2007).
11. B. P. S. Ahluwalia, W. C. Cheong, X.-C. Yuan, L.-S. Zhang, S. -H. Tao, J. Bu and H. Wang, "Design and fabrication of a double axicon for generation of tailorable self-imaged three dimensional intensity voids," Opt. Lett. **31**, 987-989 (2006).
12. G. Mikula, A. Kolodziejczyk, M. Makowski, C. Prokopowicz and M. Sypek, "Diffractive elements for imaging with extended depth of focus," Opt. Eng. **44,** 58001 (2005).

#86998 - $15.00 USD Received 29 Aug 2007; revised 17 Oct 2007; accepted 26 Oct 2007; published 13 Dec 2007

13. Z. Lu. H. Liu, R. Wang. F. Li and Y. Liu, "Diffractive axicons fabricated by laser direct writer on curved surface", J. Opt. A: Pure Appl. Opt, **9,** 160-164 (2007).
14. A. Burvall, K. Kolacz, A. Goncharov, Z. Jaroszewicz and C. Dainty, "Lens axicons in oblique illumination," Appl. Opt. **46,** 312-318 (2007).
15. S. Y. Popov and A. T. Friberg "Design of diffractive axicons for partially coherent light," Opt. Lett. **23,** 1639-1641 (1998).
16. Z. Jaroszewicz, J. F. Roman Dopazo and C. Gomez Reino, "Uniformization of the axial intensity of diffraction axicons by polychromatic illumination," Appl. Opt. **35**, 1025-1031 (1996).
17. S. Y. Popov and A. T. Friberg, "Apodization of generalized axicons to produce uniform axial line images," Pure Appl. Opt **7**, 537-548 (1998).
18. A. G. Sedukhin, "Beam-preshaping axicon focusing," J. Opt. Soc. Am. A **15,** 3057-3066 (1998).
19. J. A. Davis, C. Tuvey, O. Lopez-Coronado, J. Campos and M. J. Yzuel, "Tailoring the depth of focus for optical imaging systems using a Fourier transform approach," Opt. Lett. **32**, 844-846 (2007).
20. D. Mas, J. Garcia, C. Ferreira, L. M. Bernardo and F. Marinho, "Fast algorithms for free-space diffraction patterns calculation," Opt. Commun. **164**, 233-245 (1999).
21. D. Mas, J. Pérez, C. Hernández, C. Vázquez, J. J. Miret and C Illueca, "Fast numerical calculation of Fresnel patterns in convergent systems," Opt. Commun. **227**, 245-258 (2003).
22. C. Illueca, D. Mas, J., Perez, J. Espinosa, D. Ortiz, J. L. Alió and E. Sala, "Comparative analysis of visual performance and pseudoaccommodation between presbylasik corneas and multifocal IOL implants," J. Refract. Surg., in press (2007).
23. C. J. Zapata-Rodríguez and A. Sánchez-Losa, "Three dimensional field distribution in the focal region of low-Fresnel-number axicons," J. Opt. Am. A **23**, 3016-3026 (2006).
24. J. L. Martínez, I. Moreno and E. Ahouzi, "Diffraction and signal processing experiments with a liquid crystal microdisplay," Eur. J. Phys. **27**, 1221-1231 (2006).
25. : J. A. Davis, D. M. Cottrell, R. A. Lilly and S. W. Connely, "Multiplexed phase-encoded lenses written on spatial light modulators," Opt. Lett. **14**, 420-422 (1989).
26. Image Processing and Analysis in Java, http://rsb.info.nih.gov/ij/.
27. G. Mikula, Z. Jaroszewicz, A. Kolodziejczyk, K. Petelczyk and M. Sypek, "Imaging with extended focal depth by means of lenses with radial and angular modulation," Opt. Express **15**, 9184-9193 (2007).
28. D. Mas, J. Espinosa, J. Pérez and C. Illueca, "Scale corrections for faster evaluation of convergent Fresnel patterns," J. Mod. Opt. **53**, 259-266 (2006).

1. Introduction

Optical elements with extended depth of focus elements are of great interest that is increasing in the last few years. Several configurations are proposed in the bibliography [1-10]. Some of them are based on single elements [1,2,4,6-9,10] while others are based on convenient association of several elements [3,5,8]. Extended depth of focus in a single element is usually achieved by spatial multiplexing of phase information. We can find elements in which focusing information is codified in radial [9,11] or angular coordinates [2] or even with random localization through the surface of the element [7]. All these elements share the common property that they produce a long and narrow focal segment which allows imaging in a continuous region in the image domain. The effect can be achieved by multiplexing a continuous range of focalization distances in the element, which can be done either with refractive media [1,3,4,10] or by diffractive optical elements (DOEs) [2,6,7,9,12,13]. Among these systems, we are most interested in single diffractive structures, which can be easily implemented in a spatial light modulator (SLM). In particular we will focus our work on two particular elements: Light Sword Optical Elements (LSOE) and Fresnel Axicons (FA) Optical properties of these elements are widely known [1-3,11,15] and their performance has been optimized in several ways [16-19].

Nevertheless, we have not found many studies about performance of these elements under polychromatic illumination and none about chromatic aberrations in LSOEs. The major part of published studies are devoted to compensate chromatic aberration [5,8] or to produce on axis energy stabilization [16]. In our opinion, the special design of these elements together with polychromatic illumination lead to interesting properties in the propagated field that, to our knowledge, have not been already analyzed. Here we analyze these properties.

As it is widely known, chromatic aberration in DOEs produces an axial displacement of the light patterns. Thus, if we illuminate an input element with three different wavelengths,

#86998 - $15.00 USD Received 29 Aug 2007; revised 17 Oct 2007; accepted 26 Oct 2007; published 13 Dec 2007

we will obtain displaced colored replicas of the field distributions for each wavelength. The DOEs we have just introduced are designed to provide extended focal depth. Thus they will produce segment line whose extension is determined by the parameters of the DOE. In this communication we study the performance of these elements under chromatic illumination. We will use three different wavelengths, one per chromatic channel and we will obtain the displaced focal segments. We will explore the possibility of extending this focal segment in order to produce overlapping of the three segments. In the case of the axicon, we will show that it is possible to obtain a focal segment where all colors overlap, thus producing the effect of an achromatic axicon. In the case of a LSOE, this element produces an extra-axial segment that rotates around the optical axis. Chromatic illumination will provide presence of the three segments in the same region of the space but not axial overlapping segments. Thus, as we will show later, it is possible to obtain a range of distances where three separated focus are obtained simultaneously in the same plane. Obtaining a single element achromatic axicon could lead to new applications in instrumental optics and ophthalmology, since alignment of two compensating elements is not necessary. The LSOE in a trifocal chromatic configuration may be also used in optical information processing since it allows focusing and chromatic separation in one single element.

In this work we study chromatic aberration under different points of view. First, we will analyze on axis irradiance. This common analysis is incomplete since it does not provide full information about quality of the peak or the amount of light outside the optical axis. Therefore, we also evaluate the quality of a peak by analyzing the width of the radial MTF at each plane. Here we take profit of our previous design of fast algorithms [20-21] that compute field distributions at any propagation plane. We compute the evolution of the MTF with the propagated distance for three wavelengths. We also determine the modulation transference of the signal and the cut-off frequency of the element itself, which is of great interest if the DOE is going to be coupled to a transmittance system [22].

Finally we propose a direct exploration of all patterns. Modern computer capabilities allow composing such information and obtaining a full three-dimensional view of the light cone or even sectioning it in any plane of interest. As we will see later, this procedure provides useful information that is not affordable by other means which can be of great importance for proposing new DOEs configurations and applications. In this sense, three dimensional analysis of the field is becoming an important tool for new application designs [11,23].

2. Chromatic aberration in diffractive optical elements

Let us consider a phase-only element $u_0(\mathbf{r_0})$ where $\mathbf{r}_0 = (x_0, y_0)$ illuminated by a monochromatic plane wave whose wavelength is λ_0. Fresnel light distribution at a distance z is given by:

$$u(\mathbf{r}, z, \lambda_0) = \frac{\exp(i2\pi z/\lambda)}{i\lambda z}\exp\left(i\frac{\pi}{\lambda_0 z}\rho^2\right)\times \\ \times\int_{-\infty}^{+\infty} u_0(\mathbf{r_0})\exp\left(i\frac{\pi}{\lambda_0 z}\rho_0^2\right)\exp\left(-i\frac{2\pi}{\lambda_0 z}\mathbf{r}\cdot\mathbf{r_0}\right)d\mathbf{r_0} \tag{1}$$

where $\mathbf{r} = (x, y)$, and where $\rho = |\mathbf{r}|$, $\rho_0 = |\mathbf{r}_0|$.

As it is known if the object transmittance is not sensible to wavelength, changes in the illuminating wavelength produce the same Fresnel patterns but displaced a distance z' depending on the wavelengths ratio, i.e.:

#86998 - $15.00 USD Received 29 Aug 2007; revised 17 Oct 2007; accepted 26 Oct 2007; published 13 Dec 2007

$$
\begin{aligned}
u(\mathbf{r},z,\lambda) &= \frac{\exp(i2\pi z/\lambda)}{i\lambda z}\exp\left(i\frac{\pi}{\lambda z}\rho^2\right)\times \\
&\times\int_{-\infty}^{+\infty} u_0(\mathbf{r_0})\exp\left(i\frac{\pi}{\lambda z}\rho_0^2\right)\exp\left(-i\frac{2\pi}{\lambda z}\mathbf{r}\cdot\mathbf{r_0}\right)d\mathbf{r_0} \\
&= \frac{\exp\left(i2\pi(\lambda_0/\lambda)z/\lambda_0\right)}{i\lambda_0 z(\lambda/\lambda_0)}\exp\left(i\frac{\pi}{\lambda_0 z(\lambda/\lambda_0)}\rho^2\right)\times \\
&\times\int_{-\infty}^{+\infty} u_0(\mathbf{r_0})\exp\left(i\frac{\pi}{\lambda_0 z(\lambda/\lambda_0)}\rho_0^2\right)\exp\left(-i\frac{2\pi}{\lambda_0 z(\lambda/\lambda_0)}\mathbf{r}\cdot\mathbf{r_0}\right)d\mathbf{r_0} \\
&\equiv \exp\left(i2\pi z'\left(\frac{\lambda^2-\lambda_0^2}{\lambda_0\lambda^2}\right)\right)u(\mathbf{r},z',\lambda_0)
\end{aligned}
\tag{2}
$$

being the displacement distance z':

$$
z' = z\frac{\lambda}{\lambda_0} \tag{3}
$$

In addition, the aberrated pattern at a distance z is equivalent to the original one that was located at a distance z'. We should note that the phase factor multiplying the amplitude field does not affect both the intensity and the inner light distribution in the patterns. Therefore its presence can be ignored. Nevertheless, we will maintain it for the sake of completeness

Correction of chromatic aberration is usually done by introducing a dependence of the wavelength in the object transmittance which may compensate Fresnel displacement. Since refractive chromatic aberration has the opposite dependence of wavelength, achromatic designs combining DOEs and lenses have been widely studied (e.g. [5]). As it is outlined above here, we will design our diffractive element to produce focusing in the desired distance range for a certain wavelength λ_0 which will be called the "design wavelength". Illumination with a different wavelengths will unbalance the phases in the Fresnel integral and produce pattern displacement according to Eq. (3).

3. Chromatic displacement in axicons

Let us assume an optical element illuminated by a uniform field and let us impose that the on axis output intensity, after passing through the element, increases with z, i.e. $I_{out} = b\cdot z$. The element capable of such transformation is called a linear axicon [1]. If the structure of the element is in the form that the optical power $(1/f)$ decreases inversely with the radial coordinate (ρ), the element is called direct axicon. In this case, there is no interference between parts of the beam coming from different annular regions. This is the type of axicon that we use in this work. Since axicons are elements with rotational symmetry it is more convenient to have Fresnel integral in (2) expressed in cylindrical coordinates (ρ,θ):

$$
\begin{aligned}
u(\rho,\theta,z) &= \frac{\exp(i2\pi z/\lambda)}{i\lambda z}\exp\left(i\frac{2\pi}{\lambda z}\rho^2\right)\int_0^{2\pi}\int_0^{R_p} u_0(\rho_0,\theta_0)\times \\
&\times\exp\left[i\frac{2\pi}{\lambda}\left(\frac{{\rho_0}^2}{2z}-\frac{\rho\rho_0\cos(\theta-\theta')}{z}\right)\right]\rho_0 d\rho_0 d\theta_0
\end{aligned}
\tag{4}
$$

#86998 - $15.00 USD Received 29 Aug 2007; revised 17 Oct 2007; accepted 26 Oct 2007; published 13 Dec 2007

being R_p the aperture pupil radius.

Although the axicon is defined with a linear dependence on *z*, usually it is not needed a on axis constant growing energy along the optical axis, but the major part of it to be concentrated in a focal line along the *z* axis from distances f_0 to f_1. In this case, the following condition must be fulfilled:

$$2\pi \int_{R_1}^{R_p} I_{in}(\rho')\rho' d\rho' = \int_{f_0}^{f_1} I_{out}(z)dz \tag{5}$$

where R_1 is the inner aperture radius, and $I_{in}(\rho)$ represents the intensity transmitted by the axicon in terms of the radial coordinate, and $I_{out}(z)$ represents the intensity along the axis. With these conditions, the transmittance $T(\rho_0)$ of a direct linear axicon results [1]:

$$T(\rho_0) = \exp\left(-i\frac{2\pi}{\lambda_0}\frac{\sqrt{(1+a)\rho_0^2 + f_0^2 - aR_1^2}}{1+a}\right) \qquad \rho_0 \in \left[R_1, R_p\right]$$
$$T(\rho_0) = 0 \qquad \text{elsewhere} \tag{6}$$

being:

$$a = \frac{f_1^2 - f_0^2}{R_p^2 - R_1^2}, \tag{7}$$

We have chosen the direct linear axicon because it is of easier implementation in front of other types of axicons. Detailed discussion about performance and characteristics of the linear axicons can be found in the bibliography and will not be further discussed here.

Figure 1 shows the on-axis intensity for a linear axicon designed according to the above Eqs. (6) and (7), for three wavelengths equivalent to the Fraunhofer spectral lines, E, C',and F' which correspond to the green mercury line (λ_G=546.1 *nm*) and to the blue and red cadmium lines (λ_B=480.0 *nm*, λ_R=643.8 λ_R=643.8 *nm*). The phase transmittance of the DOE has been designed for the green color.

Results presented correspond to numerical calculations which have been done according to a far distance propagation distance algorithm presented in [20,21]. Exact parameters that have been used are summarized in Table I. All variables have been set in order that this particular design could be implemented in a standard commercial SLM. Number of samples used for this simulation is set in *N*=1024.. The closer focusing distance f_0 has been selected to be not shorter than the Nyquist focal length imposed by the size of the window. The radii R_1 and R_p have been selected as the minimum and maximum circular aperture that can be drawn in a SLM. We can see in Fig. 1 that when these elements are illuminated with polychromatic light, axicons may produce the expected displacement of the focusing region, in accordance with Eq. (3). Table 1 also indicates the values of the focusing ranges for each wavelength.

#86998 - $15.00 USD Received 29 Aug 2007; revised 17 Oct 2007; accepted 26 Oct 2007; published 13 Dec 2007

Table 1. Constants used for numerical calculations of propagated fields from DOES: λ_G corresponds to design wavelength. f_0 and f_1 are extreme distances of the focal segment, N is the number of samples used for discrete calculations. R_1 and R_p are the inner and the aperture radii of the DOE. We also show the focusing range.

DESIGN PARAMETERS					
λ_0	f_0	f_1	N	R_1	R_p
546.1 *nm*	550 *mm*	700 *mm*	1024	0.1 *mm*	6.95 *mm*
FOCUSING RANGE					
λ_R	643.8 *nm*	$f_0\lambda_0/\lambda_R$	466.5 *mm*	$f_1\lambda_0/\lambda_R$	593.7 *mm*
λ_G	546.1 *nm*	f_0	550 *mm*	f_1	700 *mm*
λ_B	480.0 *nm*	$f_0\lambda_0/\lambda_B$	625.7 *mm*	$f_1\lambda_0/\lambda_R$	796.3 *mm*

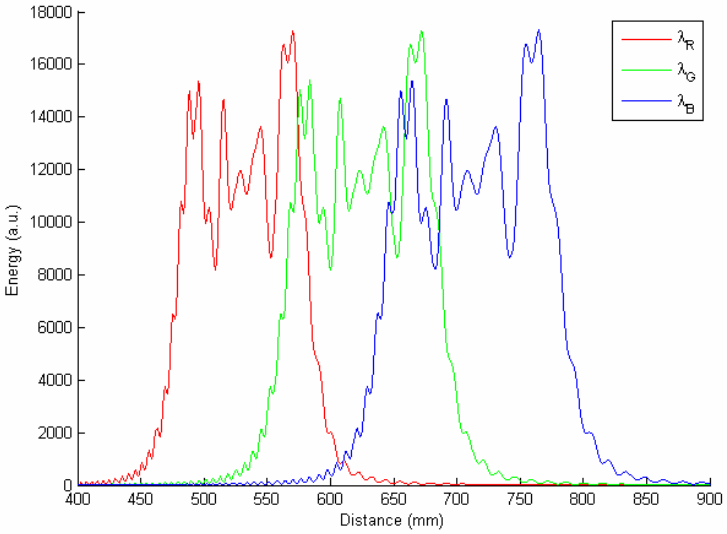

Fig. 1. Numerical simulation of on axis irradiance for a linear axicon illuminated with red, green and blue light.. The DOE has been designed for focusing in the region [f_0=550 mm, f_1=700mm] when illuminated with λ_G wavelength.

4. Achromatic axicons

As we can see in Fig. 1, when illuminated with polychromatic light, linear axicons produce colored segments displaced along the optical axis. Notice that if we extend the upper limit of the focusing line, we can achieve superposition of the three bands of color and obtain a color-balanced region between red and green and green and blue colors and even an achromatic region. The condition that must be fulfilled for obtaining an achromatic focusing region is that the two extreme colors overlap. Thus, the focal depth produced by the element must be larger than the displacement produced by the chromatic aberration. According to Eq. (3), illumination with λ_R and λ_B will displace the region to the left and to the right to $[f_0\frac{\lambda_G}{\lambda_R}, f_1\frac{\lambda_G}{\lambda_R}]$ and $[f_0\frac{\lambda_G}{\lambda_B}, f_1\frac{\lambda_G}{\lambda_B}]$ respectively. Superposition between blue and red regions will happen only while:

$$f_1\frac{\lambda_G}{\lambda_R} > f_0\frac{\lambda_G}{\lambda_B} \quad \rightarrow \quad \frac{f_1}{f_0} > \frac{\lambda_R}{\lambda_B} \tag{8}$$

#86998 - $15.00 USD Received 29 Aug 2007; revised 17 Oct 2007; accepted 26 Oct 2007; published 13 Dec 2007

Therefore, by appropriately selecting the values of f_0 and f_1 it is possible to obtain an achromatic focusing region, where all considered wavelengths are being focused. In Fig. 2, we show the effect just explained. We have selected a new range $[f_0, f_1']$ with now being $f_1' = 940\ mm$ fulfilling condition in Eq. (8) . Numerical calculation depicted in Fig. 2 show that superposition of different wavelengths produces a region where overlapping of all colors is accomplished, and then achromatism is expectable.

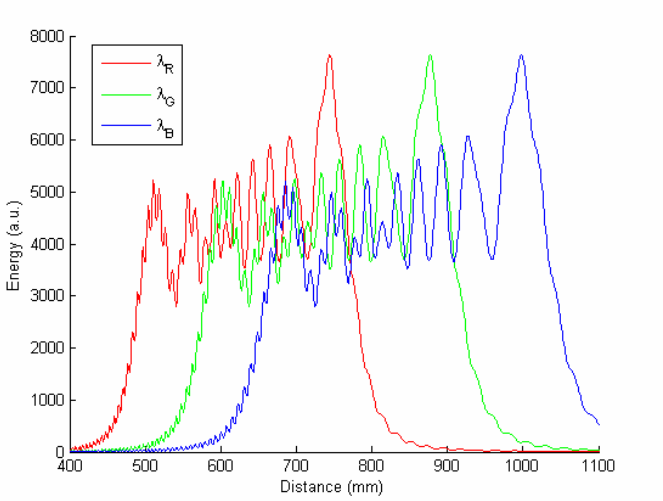

Fig. 2. Numerical simulation of on axis irradiance for a linear axicon illuminated with red, green and blue light. The DOE has been designed for green light focusing in an extended region [f_0=550 mm, f_1'=940mm] when illuminated with λ_G wavelength. Notice that superposition of colors is obtained from 650 mm to 780 mm.

Notice that in both figures axial distribution is rough. This can be corrected by introducing an apodizing filter in order to soften the axicon responses [17]. However we have preferred to present the distribution as it is and no performing additional transformations, since it does not affect to the chromatic effect we are analyzing. Notice also that the total energy peaks have diminished with respect to those represented in Fig. 1. This is a direct consequence of expanding the depth of focus of the DOE.

In order to analyze the optical quality of the achromatic region, in Fig. 3 we present the radial MTF of the light distribution in the region of interest, corresponding to an incident plane wave, for the three colors, λ_R, λ_G and λ_B. Frequency values have been normalized to the cut off value of a normal lens with the same aperture, illuminated with λ_G and focusing in the center of the interval (745 *mm*) In order to better visualize the focalization we have only represented the region up to 20% of the maximum. Values over this factor are saturated. Notice that the MTFs widen at the region where focalization is produced. We can also observe that frequency response of the element is not uniform along the focal segment, but it forms a lobe. The center of the lobe is located at the distance where we achieve the maximum MTF value. This distance coincides with the center of the focusing segment for each wavelength. We observe that there is a region where the MTF lobes for the three colors coincide. Although there is no coincidence between the maxima, we can define a band where the MTF values are balanced.

In Fig. 4 we depict the MTF for distances at the beginning, middle and end of the superposition band for the three considered wavelengths. Results are low, compared with a standard lens, but we have to consider that we are representing an achromatic depth of focus

#86998 - $15.00 USD Received 29 Aug 2007; revised 17 Oct 2007; accepted 26 Oct 2007; published 13 Dec 2007

of 120 *mm*. The result obtained here is similar to that presented in [7] by multiplexing several lenses. However, our design differs in that we obtain an achromatic focus. In addition a slow decay along the axis is observed, instead of clear peak. Since we are extending the effect of an axicon, instead of multiplexing several elements, off-axis energy is relatively low, and a more efficient element is accomplished.

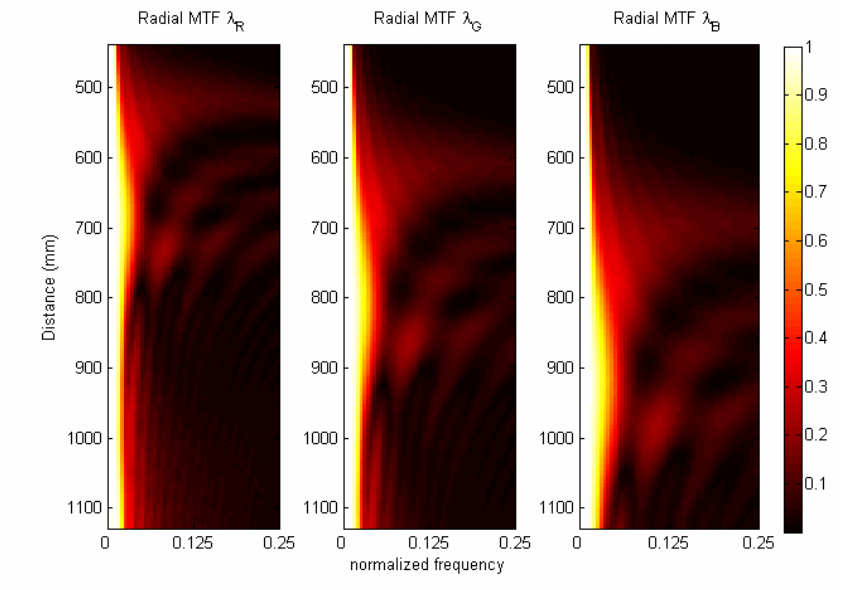

Fig. 3. Radial MTF of the linear axicon. Notice widening of the function on the region of light focalization.

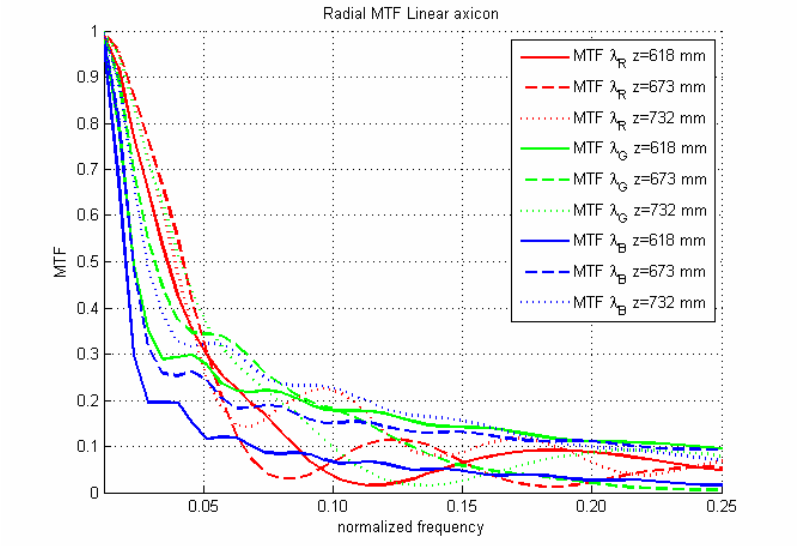

Fig. 4. Radial MTF for a linear axicon at the beginning (618 *mm*), middle (673 *mm*) and end (732 *mm*) of the region of interest. Notice that balanced MTF is obtained for three colors.

In Fig. 5, we show an animation with the RGB simulation of the 3D structure of the beam as it propagates around the region of interest. The figure has been generated by calculating the

#86998 - $15.00 USD Received 29 Aug 2007; revised 17 Oct 2007; accepted 26 Oct 2007; published 13 Dec 2007

propagated light patterns for each wavelength with the algorithm proposed in [20,21]. We have assigned the different chromatic peaks to the color RGB channels, and we have merged all the information of a plane in a single frame. Three dimensional stacking has been made with ImageJ software [26]. In order to improve the quality of the figure, we have saturated the energy at 1/3 of the absolute maximum of the obtained intensity. Even with this saturation notice that off-axis energy is relatively low. There one can also observe the structure of the achromatic region together with the other colored segments. We can see that the achromatic region is long and narrow enough to call this element an "achromatic axicon". Notice also, that if we are interested only in energy peaks, and not in chromatic components, the original extension of the axicon focal line is "chromatically" extended to a new region $\left[f_0 \ \lambda_G / \lambda_R, f_1' \lambda_G / \lambda_B \right]$.

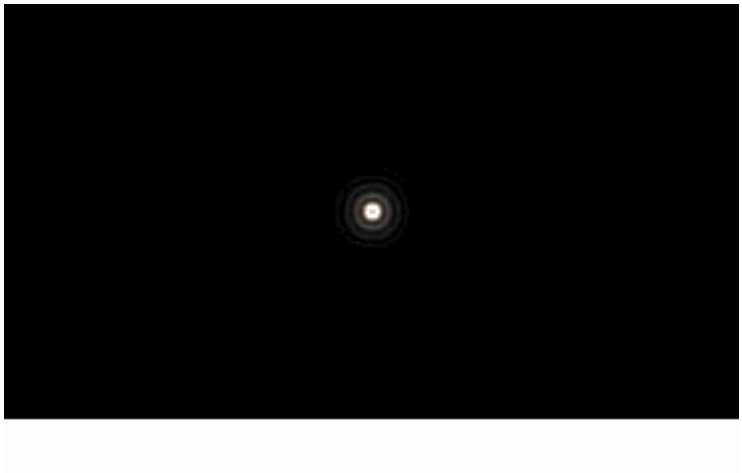

Fig. 5. Animation with the three dimensional structure of the axicon focusing segment. Notice the presence of the achromatic segment.

5. Chromatic aberration in light sword elements

In [2, 12] we find other interesting elements that produce extended depth of focus with reasonable MTF extent, which allow better contrast, but less resolution than axicons. These elements have been called Light Sword Elements (LSOE) and are based in an angular multiplexing of the convergence information and produce a comatic spot that rotates around the z-axis. In this section we apply the same chromatic analysis than in the previous case to LSOE. The transmittance function of a simple LSOE can be defined as:

$$T(\rho_0, \theta_0) = \exp\left(-i \frac{2\pi}{\lambda_0} \frac{{\rho_0}^2}{f_0 + (f_1 - f_0)\frac{\theta_0}{2\pi}} \right) \qquad \rho_0 \in \left[R_1, R_p \right], \ \theta_0 \in [0, 2\pi] \tag{9}$$

$$T_0(\rho_0, \theta_0) = 0 \qquad \text{elsewhere}$$

Notice that this transmittance is equivalent to a lens but assuming that the focal distance depends on the angle θ, i. e., for ρ_0 in the pupil region:

#86998 - $15.00 USD Received 29 Aug 2007; revised 17 Oct 2007; accepted 26 Oct 2007; published 13 Dec 2007

$$T(\rho_0,\theta_0)=\exp\left(-i\frac{2\pi}{\lambda_0}\frac{\rho_0^2}{f(\theta_0)}\right),$$
$$f(\theta_0)=f_0+(f_1-f_0)\frac{\theta_0}{2\pi} \tag{10}$$

Therefore, such element provides convergence of the beam in the region between f_0 and f_1. However, the azimuthal dependence of the phase transmittance of these elements produces off-axis shifts of the focal points. Therefore, the study of the radial MTF results is even more interesting than axial irradiance, which does not provide relevant information.

The LSOE will also be affected by chromatic aberration that may displace the peaks with respect to the design position. Again as we did in the axicon case, we impose superposition of the two extreme peaks so, from now on, we will consider the extended interval [$f_0=550$, $f_1'=940$ *mm*]. Under these conditions -polychromatic illumination and overlapping of the colored focusing zones- the particular structure of the LSOE produces interesting effects. In particular, due to the azimuthal dependence of the transmittance, the LSOE has not only lateral and longitudinal chromatic aberration, but also shows what we call "angular chromatic aberration". Consider that one beam converges, after passing through the LSOE at a distance:

$$z_1=f_0+(f_1'-f_0)\frac{\theta_0}{2\pi}. \tag{11}$$

According to Eqs. (2) and (3), illumination with a wavelength λ different from the from the design one λ_0, will produce an axial displacement of the field. Thus we will find a colored replica of the original field at a distance:

$$z'_1=\frac{\lambda_0}{\lambda}\left(f_0+(f_1'-f_0)\frac{\theta_0}{2\pi}\right). \tag{12}$$

If this displaced distance is within the range of focusing distances of the original LSOE $[f_0, f_1']$ we can advance or delay the angular coordinate θ_0 in order to move the present distribution to the same plane where original convergence was produced. The azimutal coordinate θ' that provides focusing at the same plane is given by:

$$\frac{\lambda_0}{\lambda}\left(f_0+(f'_1-f_0)\frac{\theta_0}{2\pi}\right)=\left(f_0+(f'_1-f_0)\frac{\theta'}{2\pi}\right) \tag{13}$$

And, from here we can state that illumination with two wavelengths produces, at the same plane, two different foci with an angular relative displacement between them in the form:

$$\theta'=\frac{f_0}{f_1'-f_0}\left(\frac{\lambda}{\lambda_0}-1\right)+\frac{\lambda}{\lambda_0}\theta_0 \tag{14}$$

That is what we called the "angular chromatic aberration". This effect can be better observed in Figs. 6(a) and 6(b), where an animation of the calculated light field as it propagates from 550 to 940 *mm* and the whole structure of the beam can be observed.

#86998 - $15.00 USD Received 29 Aug 2007; revised 17 Oct 2007; accepted 26 Oct 2007; published 13 Dec 2007

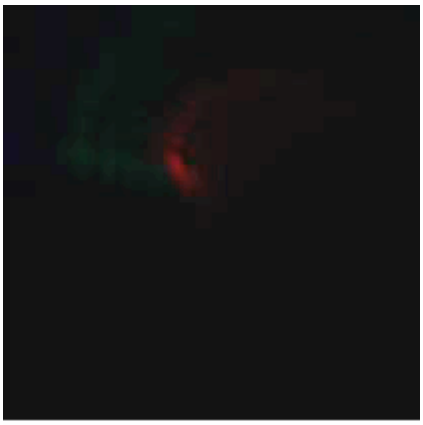

(a)

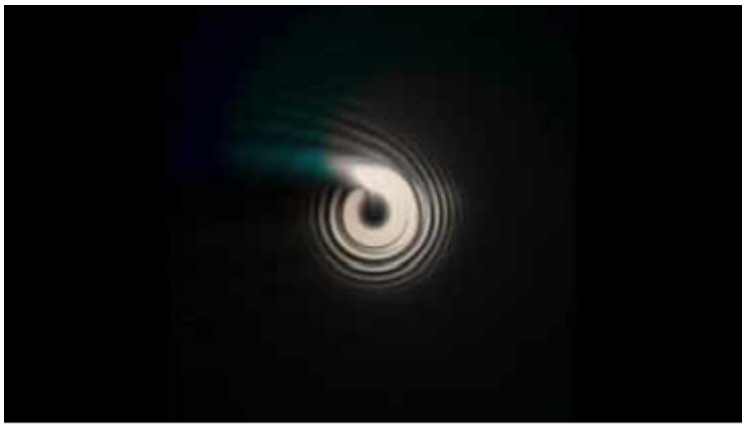

(b)

Fig. 6. Numerical simulation of on axis (a) and three dimensional structure (b) of the LSOE focusing segment. Notice the presence of three separated colored spots at a single plane.

Notice that no axial coincidence of the colors occurs at any plane. As in the previous case, the energy distributions for each color have been saturated in order to improve visualization. Unfortunately, merging the three channels causes that axial irradiance seems to be zero, although it is not.

We can also observe that it is possible to obtain three different peaks of different color simultaneously in the same plane. This fact could be used to split three color channels with one single element and without additional chromatic filter.

The quality of the three peaks can be tested by obtaining the MTF of each color separately. In Fig. 7 we show the distribution of the radial MTF along the propagation distance. We can see that the focusing region appears clearly and there is a region where superposition of the MTFs is observable. In Fig. 8 we show the MTFs at three different distances in the superposition region. We see that the MTFs are comparable for the three colors in the middle and end of the focusing region. Good balance in the entire observable region occurs only in green and red colors. It is in this region where it is possible to make

#86998 - $15.00 USD Received 29 Aug 2007; revised 17 Oct 2007; accepted 26 Oct 2007; published 13 Dec 2007

color demultiplexing of a signal. Coincidence of MTFs means that using the three colored spots for signal processing is achievable without distorting any channel with respect to other. In [27], the authors present imaging properties of LSOEs, with similar MTFs that the ones calculated here. Thus, it is possible to obtain simultaneously three different chromatic channels that can be processed together or separately.

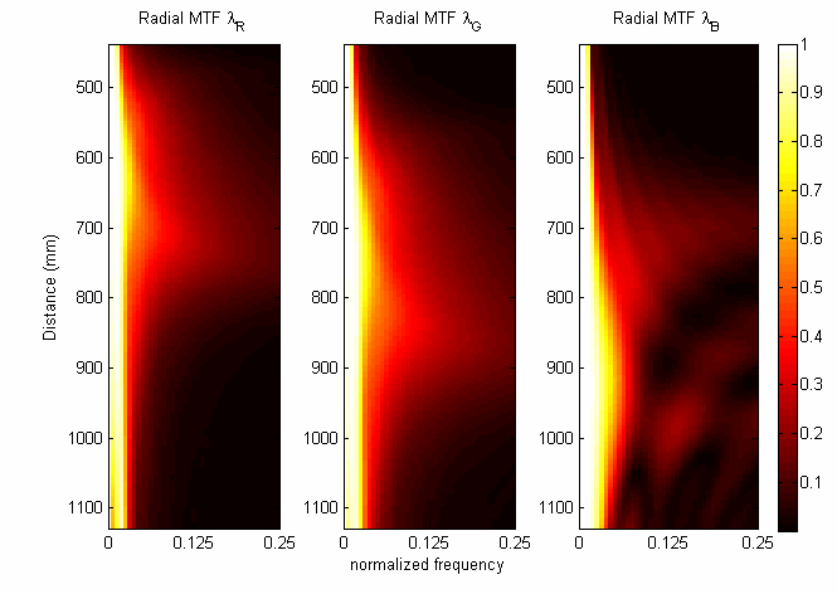

Fig. 7. Radial MTF of the linear axicon. Notice widening of the function on the region of light focalization

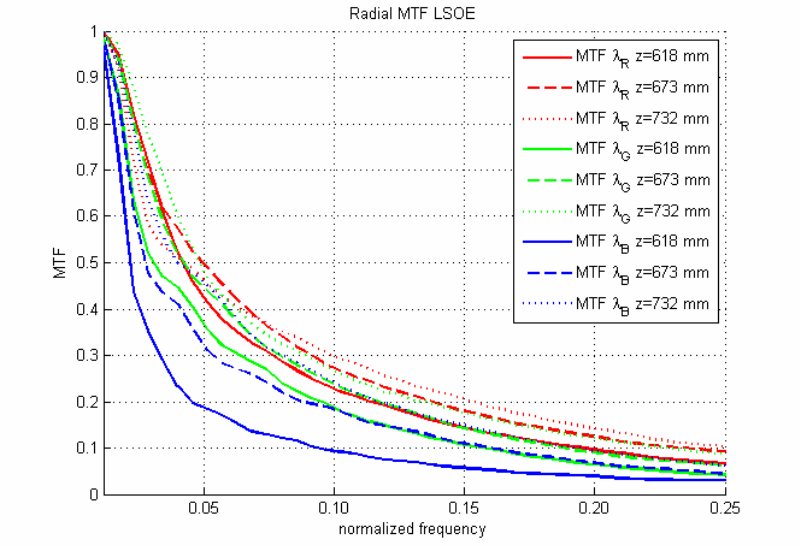

Fig. 8. Radial MTF for a LSOE at the beginning, middle and end of the region of interest.

6. Conclusions

We have analyzed the performance of two different DOEs with extended depth of focus under polychromatic illumination. We have first analyzed a linear axicon. We have showed that,

#86998 - $15.00 USD Received 29 Aug 2007; revised 17 Oct 2007; accepted 26 Oct 2007; published 13 Dec 2007

using their particular characteristics, we can extend the focusing region and force overlapping between the different chromatic segments. Superposition of the three colors λ_R, λ_G and λ_B allows obtaining an achromatic focusing region. Although the resulting element does not have a very high MTF, it may have application in designing new achromatic implants for the human eye, whose standard cutoff frequency is 0.18 times the single lens, or equivalently 30 cycles per degree [28].

We have also studied the performance of the light sword optical element (LSOE) under polychromatic illumination. It presents what we called the angular chromatic aberration, which consists in angular displacements of the same focusing spots for different wavelengths. Its particular configuration does not permit obtaining an achromatic focusing region, but allows obtaining three colored focused spots at a single plane. The MTFs analysis shows that quality of the peaks is good enough to allow their use in color signal processing, since it allows chromatic channel splitting with a single element.

Acknowledgments

This work has been financed by the Spanish Ministerio de Educación y Ciencia through the projects nr. FIS2005-05053 and FIS2006-13037-C02-02.

#86998 - $15.00 USD Received 29 Aug 2007; revised 17 Oct 2007; accepted 26 Oct 2007; published 13 Dec 2007